Design and Implementation of a Compact Master-Slave Robotic System with Force Feedback and Energy Recycling*

Chunguang LI **, Yoshio INOUE **, Tao LIU **, Kyoko SHIBATA **
and Koichi OKA **

** Kochi University of Technology
185 Miyanokuchi, Tosayamada-Cho, Kami-City, Kochi, Japan
E-mail: 126011u@gs.kochi-tech.ac.jp

Abstract

Master-slave control is becoming increasingly popular in the development of robotic systems which can provide rehabilitation training for hemiplegic patients with a unilaterally disabled limb. However, the system structures and control strategies of existent master-slave systems are always complex. An innovative master-slave system implementing force feedback and motion tracking for a rehabilitation robot is presented in this paper. The system consists of two identical motors with a wired connection, and the two motors are located at the master and slave manipulator sites respectively. The slave motor tracks the motion of the master motor directly driven by a patient. As well, the interaction force produced at the slave site is fed back to the patient. Therefore, the impaired limb driven by the slave motor can imitate the motion of the healthy limb controlling the master motor, and the patient can regulate the control force of the healthy limb properly according to the force sensation. The force sensing and motion tracking are achieved simultaneously with neither force sensors nor sophisticated control algorithms. The system is characterized by simple structure, bidirectional controllability, energy recycling, and force feedback without a force sensor. Test experiments on a prototype were conducted, and the results appraise the advantages of the system and demonstrate the feasibility of the proposed control scheme for a rehabilitation robot.

Key words: Force Feedback, Master-Slave Motion Tracking, Bidirectional Control, Energy Recycling

1. Introduction

Master-slave control schemes have attracted significant attention recently due to their wide potential applications in home-based rehabilitation robotic systems which may support home treatment of hemiplegic patients[1]-[3], teleoperation systems that enable humans to interact with remote or hazardous environments[4], and micromanipulation systems that allow humans to control objects in inaccessible microenvironments, in fields such as cell manipulation, microassembly, and microsurgery[5]-[8]. It is widely accepted that motion tracking ability in slave manipulators is essential in those systems. In addition, force feedback is also desirable since a kinesthetic feel of interaction forces can guide human operators to determine an appropriate input force according to various handling environments.

Traditionally, force feedback is realized by means of various force/torque sensors[9]-[11], which increase control complexity as well as system cost. Besides, it is extremely difficult

to mount sensors in microenvironments. W-EXOS[12] was an exoskeleton robot developed for assisting forearm and wrist motions of physically weak patients. Based on the individuals' motion intention, the robot can deliver assistance for users to perform motions of forearm pronation/supination, wrist flexion/extension and ulnar/radial deviation smoothly and naturally. However, a three axis force sensor and two torque sensors were required to obtain the force and torque information. Ueki et al[13] introduced a hand motion assist robot for independent rehabilitation therapies. With the system, the impaired hand of a patient was driven by his/her healthy hand on the contralateral side. The system was characterized by virtual reality environment displaying. The clinical tests on six patients verify that the patient's motivation for the rehabilitation was improved and enhanced. However, the force information was acquired by employing force sensors. A human-like robot hand[14] was developed with high-power and low-pressure pneumatic actuators. And a master-slave system was constructed to enable the robot hand to achieve movements in the same manner as the operator. The applied pneumatic actuators can drive the robot hand to grasp objects with enough force. However, in order to control the contact force between the robot hand and the object, a pressure sensor and a force sensor were adopted and force control was required.

On the other hand, the traditional interaction between the master and slave manipulators is always realized through the internet, which transmits control commands to the slave manipulator and the interface force in the slave site to the operator. However, few systems achieved direct electric power transmission between the master and the slave devices. That is, in order to drive the slave manipulator, a specialized power module is needed. In addition, traditional master-slave systems generally support unilateral control and the location of the master and slave devices are fixed. When the system is developed to implement rehabilitation treatment for hemiplegic patients with a unilaterally disabled limb, this is unfavorable because it is uncertain that which limb is impaired.

In this paper, we propose a new master-slave control system to realize force feedback without a force sensor and to achieve motion tracking with a kind of energy recycling. Moreover, the system can realize bidirectional control with a compact structure. As an application study, a prototype based on the control system is developed to implement rehabilitation training for hemiplegic patients with a unilaterally impaired limb.

Nomenclature

J : inertial moment

C_T : motor torque constant

R : armature resistance summation of the two motors

L : armature inductance summation of the two motors

T_0 : unload torque

T_M : motor electromagnetic torque

T : external acting torque in one terminal

e : armature voltage

i : current in the closed-loop circuit

a : rotor angular acceleration

ω : angular velocity in one terminal

θ : angular position in one terminal

N : gear ratio

η : working efficiency of the motor

α : duty cycle of the PWM signal

K_P , K_I , K_D : proportional, integral and differential coefficients

λ_T : force feedback coefficient

P_M , $P_{\sup}$, P_R : motor electromagnetic power, supplementary energy power and resistance loss power

Subscripts

m : master
s : slave

2. Methods

2.1 Master-slave system

The master-slave control system is composed of two identical motors, with the master motor being operated by a human operator and the slave motor following the master to implement the tasks commanded by the operator. The two motors have a directly wired connection and thus constitute a closed-loop circuit. The master motor as a generator powers the slave motor, which connects with a motion output terminal. An equivalent circuit diagram is shown in Fig. 1, in which M_m and M_s represent the master and the slave motors. Even though the hardware configuration at the two sites is symmetric, in order to express the slight difference in specification, the variables in the master and the slave sites are denoted with the subscripts $_m$ and $_s$ respectively.
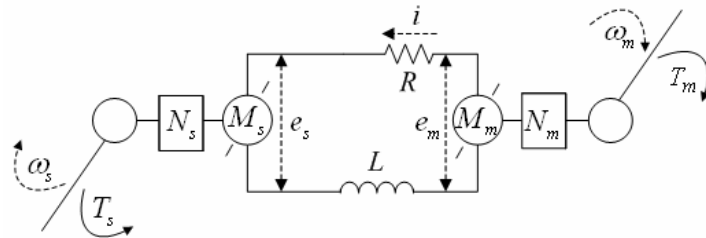

Fig. 1. Equivalent circuit diagram of the master-slave system

2.2 Theoretical formulation

Based on the dynamics mechanism, the motion equation is written as

$$\begin{cases} T_m \eta_m = (T_{M\_m} + T_{0\_m} + J_m a_m)N_m \\ T_s = (T_{M\_s} - T_{0\_s} - J_s a_s)N_s \eta_s \\ T_{M\_m} = C_{T\_m}i, T_{M\_s} = C_{T\_s}i \end{cases} \tag{1}$$

where T_m and T_s stand for the torques exerted in the two terminals; The unload torques T_{0_m} and T_{0_s} are mainly caused by mechanical friction in the motors. The electromagnetic torques of the two motors are approximately identical since the current is shared and the torque constant is much the same; Inertial torques $J_m a_m$ and $J_s a_s$ are negligible compared with other torques, thus, they are not considered in the following analysis. According to Eq. (1), the relationship between the terminal torques can be expressed as:

$$T_m = \frac{C_{T\_m} N_m}{C_{T\_s} N_s} \frac{1}{\eta_m \eta_s} T_s + \frac{N_m}{\eta_m}(T_{0\_m} + \frac{C_{T\_m}}{C_{T\_s}} T_{0\_s}) \tag{2}$$

in which the coefficients $C_{T\_m} N_m / C_{T\_s} N_s$ and C_{T_m}/C_{T_s} approximate to 1 because

the symmetric structure. Compared with the influence caused by the working efficiency of the gearboxes, the slight difference of the motors in specification is negligible. Therefore, the relationship between the terminal torques can be rewritten as:

$$T_m = \frac{1}{\eta_m \eta_s} T_s + \frac{N_m}{\eta_m}(T_{0\_m} + T_{0\_s}) \tag{3}$$

This indicates that the torques induced at the two sites correspond to each other. When the interaction force at the slave site increases, the current as well as the electromagnetic torques of the two motors increases, then, operators can sense this variation at the master site, and increase the input force accordingly to balance the torques between the two terminals. That is, based on the closed-loop current, the system is capable of implementing force feedback without using a force sensor.

Now, based on the electrical mechanism, the dynamic voltage balance equation of the master-slave circuit can be written as:

$$Ri + L\frac{di}{dt} = e_m - e_s = C_{T\_m} N_m \omega_m - C_{T\_s} N_s \omega_s \tag{4}$$

The energy generated by the master motor is transmitted to the slave motor except the

energy losses in the resistance and inductance. The coefficients $C_{T\_m} N_m$ and $C_{T\_s} N_s$

almost have no difference, thus, the master motor drives the slave motor to move with a relatively slower velocity. This means that the system has a feature of motion imitation with the energy generated by the master being recycled. Accurate motion tracking can be realized if the energy losses in the circuit are fully compensated.

2.3 Motion tracking controller

High motion tracking performance is necessary for performing rehabilitation training. However, the energy losses in the circuit make it impossible to acquire accurate motion tracking. In order to offset the energy losses in the circuit, a certain amount of energy is compensated for the circuit using an H-bridge driver. The hardware connection diagram is given in Fig. 2.

The control inputs of the H-bridge driver are a pulse-width-modulated (PWM) signal and a direction control signal, which control the magnitude and direction of the supplementary voltage respectively. Based on the velocity difference and the position difference between the two terminals, the two control signals are regulated with PID (proportional-integral-differential) control method. The motion control equation is given as:

$$\alpha = K_P^\omega((\omega_m - \omega_s) + K_I^\omega \int(\omega_m - \omega_s) - K_D^\omega \frac{d\omega_s}{dt})$$
$$+ K_P^\theta((\theta_m - \theta_s) + K_I^\theta \int(\theta_m - \theta_s) - K_D^\theta \frac{d\theta_s}{dt}) \tag{5}$$

The parameters with the superscripts ω and θ mean the coefficients related to the velocity and position respectively. Because a sudden change may happen to the velocity and position (ω_m and θ_m) that controlled by operators, the differential operation is applied only to the following velocity and position (ω_s and θ_s) rather than the velocity and

position difference so as to avoid the overshoot or fluctuation of the system. The sign and the magnitude of the control variable, α, are used to switch the direction control signal and adjust the duty cycle of the PWM signal respectively.
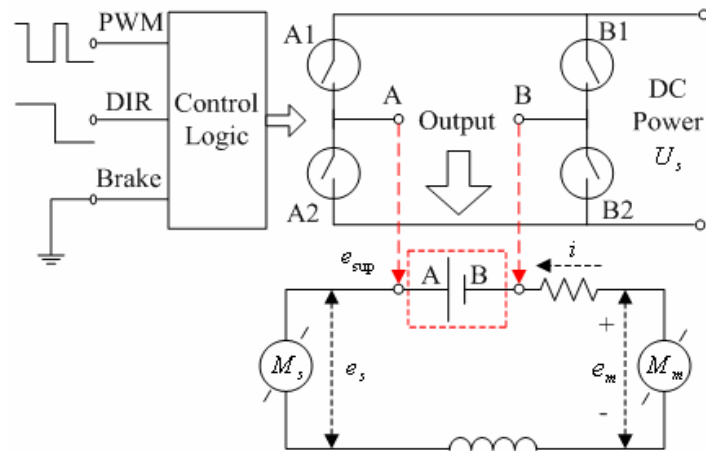

Fig. 2. Connection of the H-bridge driver and the two motors

3. Experiment Prototype

As shown in Fig. 3, a preliminary test platform was built to verify the proposed control scheme. The platform is mainly composed of two identical motor/gear units (A-max 32 motor, combined with Planetary Gearhead GP 32 A, N=4.8 and Encoder HEDL 5540, maxon, Switzerland), an H-bridge driver (LMD18200, National Semiconductor, U.S.A.), and a dSPACE control platform (CLP1104, dSPACE, Germany). In addition, two torque transducers (TP-20KCE, Kyowa, Japan) and a torque signal amplifier were applied to measure the input and output torques for verifing force feedback capability. However, they are not required in real applications.
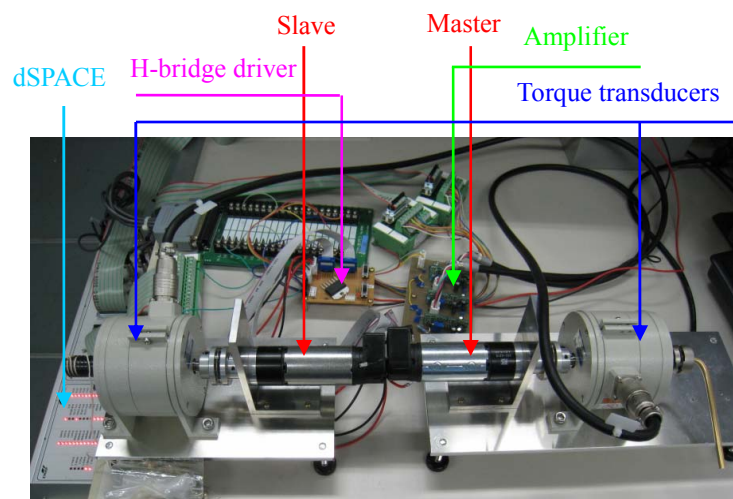

Fig. 3. Experimental platform of the master-slave system

Here, three test experiments were performed. One is force feedback test, which is used to testify the capability of force feedback and acceptable feedback performance; the second is energy recycling test, which is used to appraise the energy recycling capability of the system; the last is bidirectional control test, which is used to confirm the characteristic of bidirectional controllability and the same working performance in the two control directions.

In the first and second experiments, in order to simplify system performance analysis, a DC driving motor was used to drive the master/gear unit instead of a human operator. It was coaxially connected to the master/gear unit and was driven by another H-bridge driver, here referred to as driver 2, while the driver connected with the master-slave circuit was referred to as driver 1. The input voltage of the driving motor was adjusted based on the difference between a predefined reference velocity and the velocity in the master terminal. The schematic diagram is shown in Fig. 4. In the third experiment, an operator exerted forces on the both sides with the two hands without using the DC driving motor and the H-bridge driver 2. The corresponding diagram is shown in Fig. 5. In the figures, the master/slave unit and the motor 1/2 unit mean the combination of the motor, gearbox, encoder, and the torque transducer. The torque information given with dashed lines indicates that it is not required in real appllications.

The CLP1104 collected the velocity and position information though the incremental encoder interface, worked out the control siganls for the H-bridge driver 1 with the motion tracking controller, enabled the driver to supply a proper amount of energy for the closed-loop circuit. The energy generated by the master motor, together with the supplementary energy, drove the slave motor to track the motion of the master motor. In addition, the torque information was collected through AD modules of the CLP1104 for verifying the force feedback capability and bidirectional controllability. For the first and the second experiments, the CLP1104 also calculated the control signals for the H-bridge driver 2 and regulated the input voltage of the DC driving motor, which further rotated the system with the reference velocity. Meanwhile, the closed-loop current obtained with the H-bridge driver 1 was sampled through the AD modules of the CLP1104, and the control output of the motion tracking controller (α) was recorded for testifying the characteristic of energy recycling.
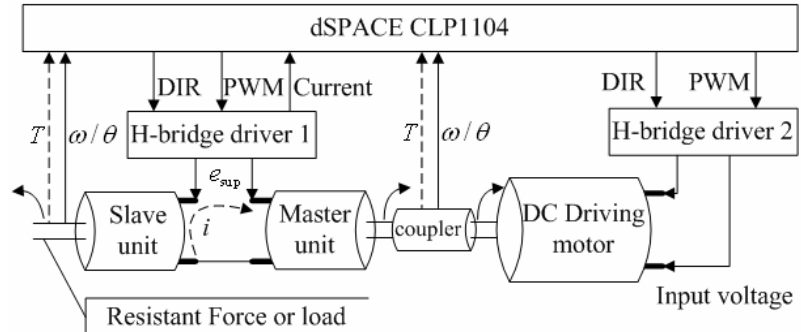

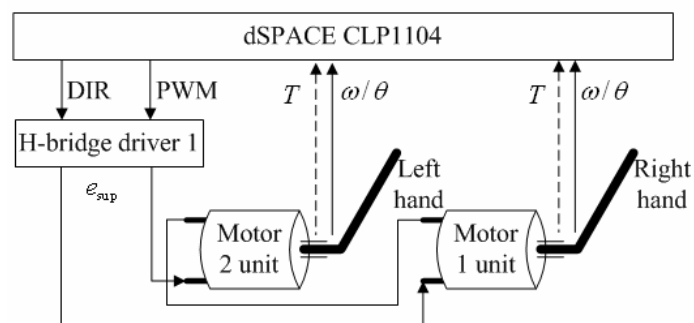Fig. 4. Schematic diagram of the experiments with DC driving motor

Fig. 5. Schematic diagram of the experiment performed with the two hands

4. Experimental Study

4.1 Force feedback test

We attached an increased resistant force to the slave site with one hand, and verified the force feedback capability based on the concomitant regulation of the force at the master site. The resistant force was intentionally exerted with a certain fluctuation so as to testify the force feedback performance. The reference velocity was set as 250 degrees/second. The tested results are given in Fig. 6, in which the opposite sign symbols denote the opposite directions of the two torques. The torque difference (T_{dif}) was the summation of the torques in the two terminals. It actually represents the difference between the two torques. In this experiment, the motion tracking was acquired with the maximum tracking errors of 2.91 degrees/second in velocity and 0.52 degree in position.
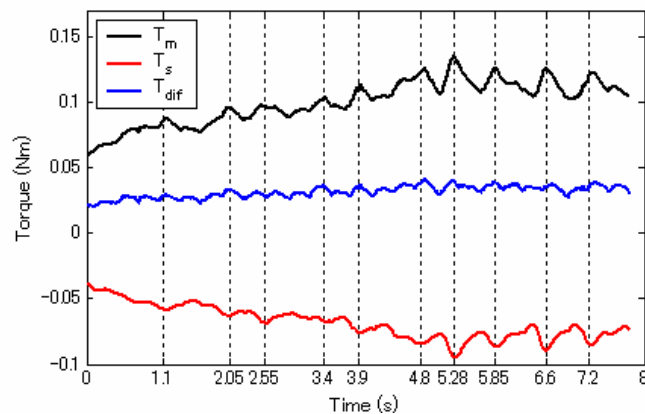
(a) Torque variation curves
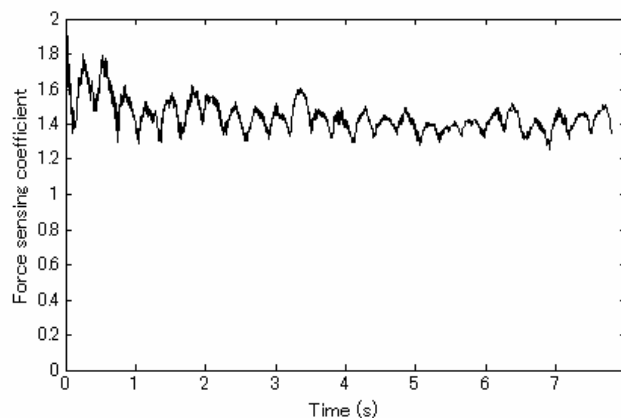
(b) Force feedback coefficient

Fig. 6. Results corresponding to the force feedback test

As shown in Fig. 6 (a), the control torque produced at the master site (controlled by the DC driving motor) increased following the increment of the resistant torque, the force feedback capability of the system is therefore demonstrated. Besides, the control torque was regulated accordingly even though the variation of the resistant torque was small, thus, good force feedback performance is confirmed. However, the control torque at the master site was larger than the resistant torque, this was caused by the unload torques of the motors and the frictional torques induced by the gearboxes (working efficiency). Although there was a difference in the torques, the force feedback capability can assure the operator to regulate the control force in the master site accurately according to the resistance variation in the slave site. In addition, the torque difference kept nearly constant even though the forces

exerted in the two terminals were increased. This indicates that the varying external acting force had unnoticeable impact on the unload torques and gearboxes' frictional torques so long as the rotational velocities were kept constant. It is true that the torque difference (mainly caused by the working efficiency of the gearboxes) will change slightly following the variation of the velocity, whereas the operator can sense this variation and regulate the control force according to the expected rotational velocity. In the considering application, the variation of the torque difference is very small compared to the variation of the external resistance. Furthermore, the system is mainly aimed at achieving motion tracking and the force transparency is less essential. Therefore, the torque difference is acceptable for the considering system.

In order to quantify the force feedback capability of the system towards the external impedance variation at the slave site, we defined force feedback coefficient as:

$$\lambda_T = \frac{\Delta T_m}{\Delta T_s} = \frac{T_m^k - T_m^0}{T_s^k - T_s^0} \qquad (6)$$

where T_s^0 and T_m^0 represent the initial torques when there was no external resistant force and the system was rotated with the velocity of 250 degrees/second. T_s^0 (0.032 Nm) was used to drive the worm gear at the slave site. T_m^0 (0.048 Nm) was used to overcome the frictional torques in the gearboxes and the unload torques in two motors, further to drive the two motors to rotate; the variables with the superscript k denote the sampling values in the k time. The initial torques were excluded in the calculation for eliminating the effect of unload torques. The force feedback coefficient curve is shown in Fig. 6 (b), the system realized force feedback with an approximately constant reflecting coefficient. The average coefficient was 1.445. It was larger than the unit one, the cuase of this is considered to be the frictional torques induced by the gearboxes. In order to reduce the requirment for the control force and enhance force presence performance, the motors and gearboxs with higher working efficiencies should be employed.
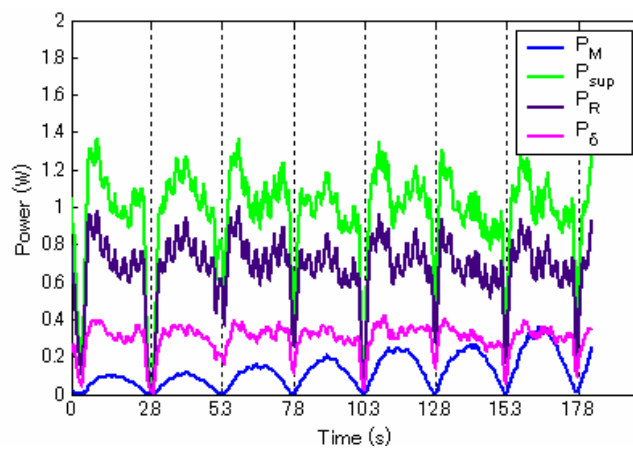
4.2 Energy recycling test

Even though the energy generated by the master is recycled by the slave motor, as expressed in Eq. (4), the energy loss in the circuit makes the velocity of the slave motor is slower than that of the master motor. Therefore, we compensated a certain amount of energy to offset the energy loss in the circuit. In order to verify the energy recycling capability, the reference velocity was set as a sine signal with an increasing magnitude in different periods. That is, the system was rotated with clockwise and counter-clockwise direction periodically. No external load was attached to the slave site. The electromagnetic power, supplementary energy power, and the power of the resistance loss were calculated with:

$$\begin{cases} P_M = C_{T\_s} i N_s \omega_s = i e_s \\ P_{\sup} = \alpha U_s i \\ P_R = i^2 R \end{cases} \qquad (7)$$

where U_s denotes the supply voltage of the H-bridge driver. U_s was 12 volts and R was 6.04 ohms. Since $\omega_m = \omega_s$ when the system achieved motion tracking and the system was configured with a symmetrical structure (the corresponding coefficients in the two sites are almost identical), P_M represented the electromagnetic power of the two motors actually. The inductance loss was not considered because that it was very small and negligible compared to the resistance loss. The electromagnetic power and the supplementary energy power were used to verify the energy recycling capability; the supplementary energy power and the resistance loss were used to confirm the function of the supplementary energy.
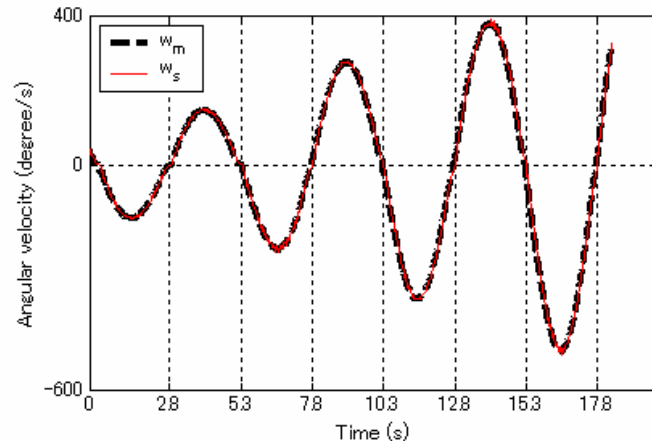
(a) Velocity tracking curves

(b) Relationship between the motor electromagnetic power,
supplementary energy and the resistance loss

Fig. 7. Results corresponding to the energy recycling test

The results corresponding to the energy recycling test are given in Fig. 7, in which P_δ denotes the power difference between the compensated energy and resistance loss. Seeing Fig. 7 (a), it can be concluded that accurate motion tracking was realized in both rotational directions. In this test, the maximum velocity and position errors were 4.06 degrees/second and 0.5 degree respectively. As can be seen from Fig. 7 (a) and (b), the electromagnetic power of the slave motor (represents the electromagnetic power of the two motors) increased with the variation of the velocity (The powers were always positive even though the velocity was negative), whereas the compensated energy had unnoticeable changes among different periods. This indicates that the driving power of the slave motor came from the electric energy generated by the master motor other than the compensated energy. Hence, the energy recycling capability is confirmed. Meanwhile, the compensated energy and the resistance loss had the same varying regulation in each period, this demonstrates that the compensated energy was used to offset the energy losses in the circuit. However, the former was larger than the latter because there were also inductance loss, as well as the contact loss and excitation loss that are caused by the armature current and alternative magnetic field. The resistance loss accounted a main part of the energy losses and thus, P_R was relatively large compared to P_δ, which reflected the power of the other energy losses in the circuit.

However, the compensated energy was larger than the electromagnetic power of the slave motor because of the large energy losses in the circuit. In order to reduce the energy

losses in the circuit and enhance energy recycling efficiency, the motors with a smaller armature resistance should be considered in the future applications.

4.3 Bidirectional control test

The force feedback mechanism and the symmetric configuration make the system have the characteristic of bidirectional controllability. In order to verify this feature, the DC driving motor that controlled the master/gear unit and the H-bridge driver 2 were removed from the experimental platform. An operator controlled the acting forces on the both sides with the two hands. The exerted forces had opposite directions and different magnitudes with the smaller one defined as the resistance force and the larger one defined as the control force, and the two motors in the corresponding sides behave as the slave and the master respectively. During the experiment, the operator changed the magnitude of the resistant force periodically and regulated the control force according to the feedback force, trying to achieve a movement with small variation among different periods.

The results coresponding to the two control directions are shown in Fig. 8 and Fig. 9 respectively. Fig. 8 gives the results of the test when the right hand provided a control force while the left hand imposed a resisitant force with relatively small magnitudes. That is, the motor located at the right hand site acted as the master while the other motor acted as the slave; Fig. 9 gives the results of the test when the left hand provided a control force while the right hand imposed a resisitant force with relatively small magnitudes, and the working states of the two motors were reversed compared to the former case. In the both figures, the black line represents the torque produced on the right hand side and the the red line represents the torque produced on the left hand side, the blue line represents the difference between the control torque and the resistant torque in the two terminals.

It can be seen that the accurate motion tracking was achieved in the both control directions. The maximum veloity and position errors were 11.67 degrees/second and 0.77 degree when the control direction was from right to left, and were 16.88 degrees/second and 0.41 degree when the control direction was from left to right. In addition, the control torque increased following the increment of the resistant torque in the two control directions. This confirms that force feedback/sensing was realized in the both control directions and the operator was able to regulate the control force accordingly based on the sensation of the feedback force. Besides, by comparing Fig. 8 (c) and Fig. 9 (c), it can be concluded that when the resistant torques had the same magnitude (0.078 Nm), the control torques (0.115 Nm) as well as the torque differences (0.037 Nm) were approximately indentical for the two control directions. The resluts verify that the system implemented bidirectional control and achieved almost the same force feedback performance for the both control directions. As well, the relationship between the control torque and the resistant torque are given in Fig. 8 (d) and Fig. 9 (d). We can see that there were hysteretic errors when the reciprocating motion was carried out for the both control directions. When the resistant torque was small, the unload torques of the motors and the frictional torques caused by the gearboxes were too large compared to the resistant torque, thus the hysteretic errors were obvious. In the testing range of the resistant force, the average hysteretic deviations are 0.0051 Nm and 0.012 Nm respectively; and the standard deviations are 0.0092 and 0.015 respectively for the two control directions.

When we apply this master-slave system to a rehabilitation robot for training hemiplegic patients, the bidirectional controllability allows the system to provide treatments for patients no matter which limb is disabled or has weak motor function. Therefore, the proposed master-slave system is preferrable for a rehabilitation robot to provide treatments for hemiplegic patients with a unilaterally disabled limb.
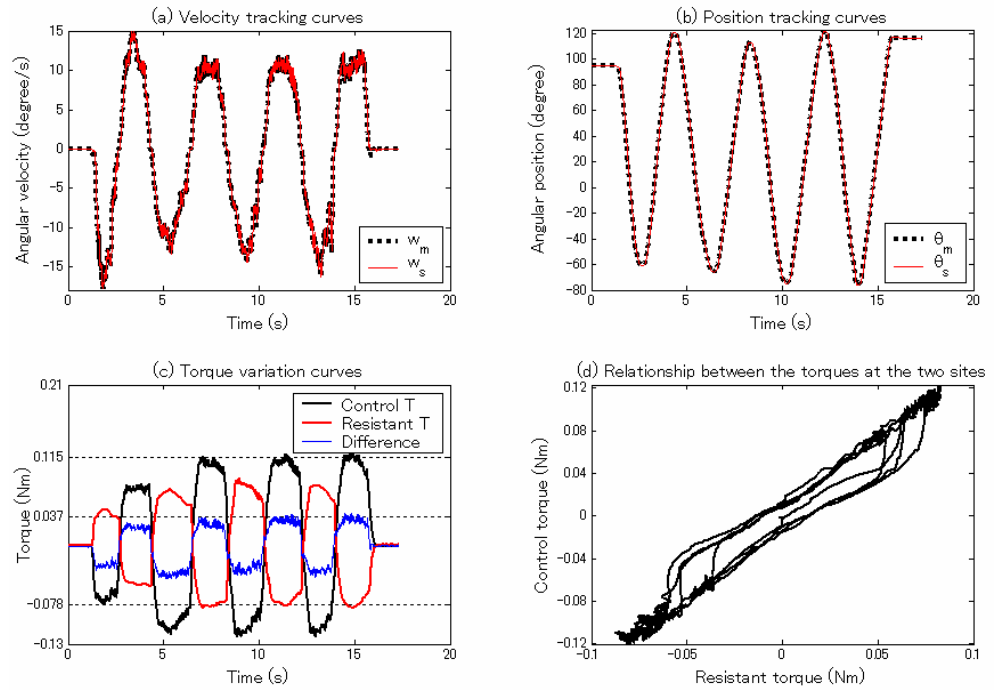
Fig. 8. Results of the test when the right hand controls the movements of the left hand
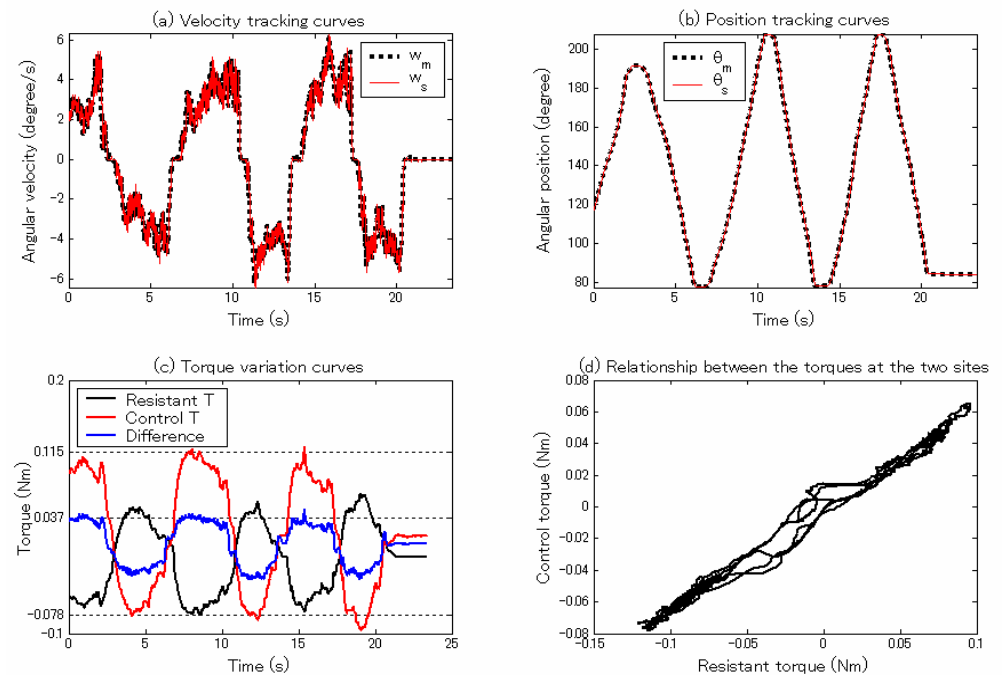
Fig.9. Results of the test when the left hand controls the movements of the right hand

5. Conclusion

A new master-slave robotic system is proposed to achieve motion imitation. The system realizes bidirectional control and has the capability of force feedback and energy recycling. A prototype was set up and verification experiments were performed. The experimental results demonstrate the feasibility of the proposed control system for developing a rehabilitation robot.

In our new system, the motion tracking capability makes it possible for hemiplegic patients to perform unassisted rehabilitation training in the home environment with the unhealthy limb imitating the motion of the healthy limb. Force feedback can give patients a direct sensation of the resistant forces produced by the impaired limb, thus enabling the healthy limb to provide a proper control force and avoid unpredictable reactions. The force feedback is realized without a force sensor; hence, the system structure and the control method are simplified greatly. Energy recycling makes a lightweight battery can supply enough power for the system, further to reduce the weight of the robot. This is especially favorable for patients wearing a portable robot so as to move around freely. Bidirectional controllability makes the system have no limitation in hardware configuration, which enables the robotic system to deliver treatment for hemiplegic patients no matter which limb is impaired. In conclusion, the proposed system is favorable to realize self-controlled rehabilitation robot for training hemiplegic patients in motor function recovery and strength enhancement.

However, there are still some limitations for the new system. The force feedback performance will be degraded when the velocities have a large variation. This is especially the case when the motors have large unload torques and the gearboxes have large gear ratios. Thus, the system is only suitable for the applications without obviously varying velocity. In future study, motors and gearboxes with higher working efficiencies will be considered to reduce the above negative effect. As for the preliminary experimental prototype, the proportional, integral and differential coefficients of the motion tracking controller were just coarsely regulated. The motion tracking precision will be enhanced by further regulating the coefficients. In addition, motor/gear combination with larger driving torque/power may be selected to make the system more suitable for a rehabilitation robot.

References

(1) Peng, Q., Park, H.-S., Zhang, L.-Q., 2005, "A Low-Cost Portable Tele-Rehabilitation System for the Treatment and Assessment of the Elbow Deformity of Stroke Patients," *Proc. 2005 IEEE 9th Int. Conf. on Rehabilitation Robotics,* Chicago, Illinois, 28 June-1 July, pp.149- 151.

(2) Li, H., Song, A., 2008, "Force assistant master-slave telerehabilitation robotic system," J. Southeast University, **24**(1), pp. 42-45.

(3) Schiele, A., Letier, P., Van Der Linde, R., Van Der Helm, F., 2006, "Bowden cable actuator for force-feedback exoskeletons," in *IEEE Int. Conf. Intelligent Robots and Systems,* Beijing, China, pp. 3599-3604.

(4) Alfi, A., Farrokhi, M., 2008, "Force reflecting bilateral control of master-slave systems in teleoperation," J. Intelligent and Robotic Systems: Theory and Applications, **52**(2), pp. 209-232.

(5) Ephanov, A.V., Hurmuzlu, Y., 1997, "Implementation of sensory feedback and trajectory tracking in active telemanipulation systems," J. Dyn. Syst., Meas., Control, **119**(3), pp. 447-454.

(6) Vlachos, K., Vartholomeos, P., Papadopoulos, E., 2007, "A haptic tele-manipulation environment for a vibration-driven micromechatronic device," in *IEEE/ASME Int. Conf. on Advanced intelligent mechatronics,* pp. 1-6.

(7) Ando, N., Korondi, P., Hashimoto, H., "Development of micromanipulator and haptic interface for networked micromanipulation," *IEEE Trans. Mechatron.,* IEEE-INST ELECTRICAL ELECTRONICS ENGINEERS INC, **6**(4), pp. 417-427.

(8) Gorman, J.J., Dagalakis, N.G., 2006, "Probe-based micro-scale manipulation and assembly using force feedback," presented at the 1st Joint Emergency Preparedness and Response/Robotic and Remote Systems Topical Meeting, pp. 621-628.

(9) Mitsuishi, M., Sugita, N., Pitakwatchara, P., 2007, "Force-feedback augmentation modes in the laparoscopic minimally invasive telesurgical system," *IEEE/ASME Trans. Mechatronics,* **12**(4), pp. 447-454.

(10) Lee, Sukhan, Lee, Hahk Sung, 1993, "Modeling, design, and evaluation of advanced teleoperator control systems with short time delay," *IEEE Trans. Robot. Autom.,* **9** (5), pp. 607-623.

(11) Hara, M., Huang, J., Jung, Y.-M., Yabuta, T., 2006, "Basic Study on Sensory Aspects of a Master/Slave System for Force Telecommunication," *in Int. Conf. on Intell. Robots Syst.* Beijing, China, 9-15 Oct., pp. 1706-1711.

(12) Ranathunga Arachchilage Ruwan Chandra GOPURA, Kazuo KIGUCHI, 2008, "An Exoskeleton Robot for Human Forearm and Wrist Motion Assist," *Journal of Advanced Mechanical Design, Systems, and Manufacturing,* **2**(6), pp.1067-1083.

(13) Ueki, S., Nishimoto, Y., Abe, M., Kawasaki, H., Ito, S., Ishigure, Y., Mizumoto, J., Ojika, T., 2008, "Development of virtual reality exercise of hand motion assist robot for rehabilitation therapy by patient self-motion control," *in IEEE Int. Conf. on Eng. Med. Biol. Soc.,* pp. 4282-4285.

(14) Nobutaka TSUJIUCHI, Takayuki KOIZUMI, Shinya NISHINO, Hiroyuki KOMATSUBARA, Tatsuwo KUDAWARA, Masanori HIRANO, 2008, "Development of Pneumatic Robot Hand and Construction of Master-Slave System," *Journal of System Design and Dynamics,* **2**(6), pp.1306-1315.